GEOPHYSICS. VOL. 76, NO. 5 (SEPTEMBER-OCTOBER 2011); P. WB183–WB190, 11 FIGS.
10.1190/GEO2010-0395.1

DOI:10.1190/geo2010-0395.1

Multiparameter joint tomography for TTI model building

Chaoguang Zhou[1], Junru Jiao[1], Sonny Lin[1], John Sherwood[1], and Sverre Brandsberg-Dahl[1]

ABSTRACT

Model building for tilted transversely isotropic media has commonly been performed by a single parameter tomography that updates the velocity in the symmetry direction, while the orientation of the symmetry axis and Thomsen parameters ϵ and δ are typically estimated from the migration stack and well data. Unfortunately, well data are often not available. In addition, when they are available, their lateral sampling is typically very sparse and their vertical sampling usually spans only a limited range of depths. In order to obtain spatially varying anisotropic models, with or without well data, we developed a multiparameter joint tomographic approach that simultaneously inverts for the velocity in the symmetry axis direction, ϵ and δ. We derived a set of reflection tomography equations for slowness in the symmetry axis direction and Thomsen parameters ϵ and δ. In order to address the nonuniqueness of the tomography, we developed a regularization strategy that uses an independent regularization operator and regularization factor for each individual anisotropy parameter. Synthetic tests found that ambiguity exists between the anisotropy parameters and that velocity has a better resolution than ϵ and δ. They also confirmed that joint tomography provides a better data fit than single parameter tomography. The field example was used to test a way to incorporate the sonic data in the model building process and limit the tomographic updates on certain anisotropy parameters by adjusting the regularization.

INTRODUCTION

In many areas throughout the world, accurate imaging in depth requires an anisotropic representation of earth parameters (Alkhalifah and Larner, 1994; Bear et al., 2005; Bowling et al., 2009; and Schleicher et al., 2010). In many cases, the anisotropic effects on recorded data can be adequately explained by hexagonal elastic symmetry. This type of anisotropy is referred to as *tilted transverse isotropy*, or *TTI*, and is characterized by three anisotropy parameters, the velocity in the symmetry axis direction, and Thomsen parameters ϵ and δ, along with the orientation of the symmetry axis (Thomsen, 1986). When the symmetry axis is vertical, the resulting anisotropy is referred to as *vertical transverse isotropy*, or *VTI*.

A number of approaches have been suggested in order to estimate these anisotropy parameters. Tsvakin and Thomsen (1995), Alkhalifah and Tsvankin (1995), and Grechka and Tsvankin (1998) analyze NMO moveout and determine an "effective η," which is a parameter defined by ϵ and δ, and NMO velocity in order to improve images in the time domain. The resulting velocity and η values can then be converted to interval velocity and η values versus depth by using an extended Dix formula.

In recent years, several approaches to direct estimation of anisotropy parameters in the depth domain have been developed. One category of those approaches consists of several steps that solve for each anisotropy parameter separately, using the surface seismic data with or without the well information. Bear et al. (2005) separately estimate anisotropy parameters for VTI media by using information from surface seismic, check-shot, and sonic data. The procedure starts at the well locations. First the vertical velocity is determined by matching modeled traveltimes to observed vertical check-shot or sonic data. The anisotropic parameter δ is then adjusted to flatten the near- to mid-offsets of the migrated seismic gathers at the well locations. The parameter η is finally picked to remove the remaining moveouts at far offsets. Parameters δ and η can be further adjusted if offset check-shot data are available. A 3D interpolation is then used to create anisotropic models for imaging. Woodward et al. (2008) apply a multistep approach, in which an isotropic P velocity is first obtained by standard grid tomography and then scaled to tie the well. The Thomsen parameters ϵ and δ are estimated by interactive 1D forward modeling to flatten gathers at the well. The 1D δ function then is extended horizontally as a constant away from the well while the ϵ function is extended to be consistent with the laterally varying η field derived from the time

Manuscript received by the Editor 30 November 2010; revised manuscript received 29 April 2011; published online 21 November 2011.
[1]Petroleum Geo-Services, Houston, Texas, U.S.A. E-mail: chaoguang_zhou@hotmail.com; junru.jiao@pgs.com; sonny.lin@pgs.com; John.Sherwood@pgs.com; Sverre.Brandsberg-Dahl@pgs.com.

processing. Koren et al. (2008) develop a local tomography method that estimates δ from short-offset events and ε from long-offset data.

Another popular category is single parameter tomography. Estimates are somehow made for ε and δ at well locations and are interpolated over the entire model volume to provide final ε and δ models, with the velocity then being updated iteratively, just as in isotropic tomography. Schleicher et al. (2010) describe a TTI model building method that includes calibrating seismic depths to well depths to obtain δ and ε, estimation of the symmetry axis of the anisotropy, and iterative depth migration and tomography to update the velocity in the symmetry axis direction. Huang et al. (2007) propose a joint inversion of ε and δ at the well location where the vertical velocity is obtained from calibration with check-shot data. Then the 1D ε and δ functions are hung from the water bottom to generate 3D volumes. The 3D ε and δ volumes are fixed thereafter, and single parameter tomographic updates are estimated for the vertical velocity. This approach is also applied by Bowling et al. (2009) on wide azimuth data. Bakulin et al. (2010a, 2010b) develop a local approach that inverts for anisotropic parameters by using surface seismic and check-shot data and a horizon-guided interpolation in order to generate 3D anisotropy parameter volumes.

Several studies have also been conducted on the joint estimation of anisotropy parameters from seismic data. Cai et al. (2009) employ a focusing analysis for estimating anisotropy parameters in both time and depth domains. Zhou et al. (2003) propose a 3D tomo graphy that simultaneously inverts for anisotropy parameters. The tomography equations are derived for the velocity in the symmetry direction, ε, and δ under the assumption of weak anisotropy. A similar study also is done by Jiang et al. (2009) for 2D TTI media.

In this article, we present a multiparameter joint tomography method for TTI model building. Our work is motivated by the observation that well information is only sparsely available and is thus incapable of providing models with high lateral resolution. In frontier areas, there may not be any well data available at all. We also believe that a simultaneous inversion for several parameters has the potential to yield a better data fit than single parameter tomography or multistep schemes. Seismic reflection tomography is an underdetermined inversion problem. To constrain such an inversion, Tikhonov and Arsenin (1977) introduce regularization by adding a term in the minimization objective function to give preference to a particular solution with desirable properties. A differentiation (roughening) operator is typically used in the regularization term. Harlan (1995) reparameterizes it into another form by introducing a smoothing operator. The multiparameter tomography is even more underdetermined because we have to invert for more parameters. Bakulin et al. (2010a) show that even 1D inversion for TTI parameters at the well location using both surface seismic and well data is nonunique. Moreover, each anisotropy parameter may have a different spatial variation. To address these issues, we develop a regularization scheme that accommodates independent spatial variations for the anisotropy parameters and gives users some leverage to control the back-projection of the tomography.

THEORY

Tomography equations

The phase velocity for seismic P waves in anisotropic media is a complex function of the anisotropy parameters discussed earlier and the velocity for shear waves (Thomsen 1986, Tsvankin, 2001). Alkhalifah (1998) and Tsvankin (2001) show that the influence of the shear-wave velocity on the P wave velocity is practically negligible for all anisotropic media. By setting the shear velocity to zero, the P wave phase velocity can be simplified to

$$V(V_{p0},\theta,\varepsilon,\delta) = V_{p0}\sqrt{0.5+\varepsilon\sin^2\theta+0.5\sqrt{(1+2\varepsilon\sin^2\theta)^2-8(\varepsilon-\delta)\sin^2\theta\cos^2\theta}}, \quad (1)$$

where V_{p0} is the phase velocity along the symmetry axis; θ is the angle between the slowness vector and the symmetry axis; and ε and δ are Thomsen parameters.

The traveltime in a finite model cell is the group slowness multiplied by the travel distance. Because the phase velocity is the projection of the group velocity (Tsavnkin, 2001), the traveltime can be expressed as

$$t = gl = sl\cos\phi, \quad (2)$$

where g is the group slowness; l is the distance propagated; s is the phase slowness; and ϕ is the angle between the phase slowness vector and the group slowness vector. By applying the first order Taylor expansion, the traveltime changes due to changes in the model, in the context of linear tomography, can be expressed approximately as

$$\Delta t = \frac{\partial \mathrm{t}}{\partial \mathrm{s}_{p0}}\Delta s_{p0}+\frac{\partial \mathrm{t}}{\partial \varepsilon}\Delta\varepsilon+\frac{\partial \mathrm{t}}{\partial \delta}\Delta\delta = \left(\frac{\partial \mathrm{s}}{\partial \mathrm{s}_{p0}}\Delta s_{p0}+\frac{\partial \mathrm{s}}{\partial \varepsilon}\Delta\varepsilon+\frac{\partial \mathrm{s}}{\partial \delta}\Delta\delta\right) l\cos\phi, \quad (3)$$

where s_{p0} is the slowness along the symmetry axis. Although the traveltime change is a function of the orientation of the symmetry axis too, we omit it in equation 2 for the sake of simplicity. Under some circumstances, the orientation of the symmetry axis can be approximated by setting its direction to be normal to the structure. This is accomplished by scanning the dips of the sediment bedding and then orienting the symmetry axes orthogonal to the bedding. The special TTI medium with such symmetry axis orientation is referred to as the Structurally Conformable TTI (STI) medium. Audebert et al. (2006) show that STI dips can be adequately determined by means of VTI elliptic, or even isotropic migrations.

From equation 1, we can derive the derivatives of the slowness

$$\frac{\partial s}{\partial s_{p0}} = r, \quad (4)$$

$$\frac{\partial s}{\partial \varepsilon} = -0.5 s_{p0} r^3[1+\rho(1+2\varepsilon\sin^2\theta-2\cos^2\theta)]\sin^2\theta, \quad (5)$$

$$\frac{\partial s}{\partial \delta} = -s_{p0} r^3 \rho \sin^2\theta\cos^2\theta, \quad (6)$$

$$r = \left[0.5+\varepsilon\sin^2\theta+0.5\sqrt{(1+2\varepsilon\sin^2\theta)^2-8(\varepsilon-\delta)\sin^2\theta\cos^2\theta}\right]^{-1/2}, \quad (7)$$

$$\rho = 1/\sqrt{(1+2\varepsilon\sin^2\theta)^2 - 8(\varepsilon-\sigma)\sin^2\theta\cos^2\theta}. \quad (8)$$

A similar set of formulas can be found in Jiang et al. (2009) and Zhou et al. (2003) for weak anisotropic media. For consistency in the dimensions of parameters, it is preferred to invert for Δs_{p0}, $s_{p0}\Delta\epsilon$, and $s_{p0}\Delta\delta$ and then derive $\Delta\varepsilon$ and $\Delta\delta$, resulting in an updated model for V_{p0}, ε, and δ.

Ray tracing and equation setup

All traveltime derivatives with respect to slowness, ε and δ are calculated through TTI ray tracing. To do that, the common reflection points and their dips are automatically picked from the initial migration stack while the corresponding depth residual moveouts are derived from the migration gathers (Jiao et al., 2009). Specular ray pairs are traced from the picked common reflection points through the anisotropic model to all source and receiver locations at the surface. As described in Zhou et al. (2003), a special numerical solver is employed to find the reflection angle according to Snell's law. All time derivatives in equation 3 are calculated during ray tracing along the raypaths for each specular ray pair. The traveltime change due to the reflector shift (Zhou et al., 2003) is a function of the phase velocities of the incident ray and reflected ray, the angle of incidence and the angle of reflection. Because we only measure residuals in the depth direction, the z component of the slowness vector $\frac{\partial t}{\partial z}$ (Koren et al., 2008) at the common reflection point is used to convert the corresponding depth residual to the time residual Δt in equation 3. The true depth residual moveout corresponding to a specular ray pair consists of the residual, with respect to the current depth of the common image point, plus the unknown difference between the true depth and the current depth of the common image point. Because this unknown difference exists in all equations that are set up at a common reflection point, it can be eliminated by subtracting one equation, usually corresponding to the near offset, from all others (Zhou, et al., 2008; Kosloff, et al., 1997; Koren et al., 2008).

Thus, we set up the tomography system as

$$\mathbf{Ax} = \mathbf{b} \quad (9)$$

where $\mathbf{x}$ is a vector of parameter perturbations Δs_{p0}, $s_{p0}\Delta\epsilon$, and $s_{p0}\Delta\delta$; matrix $\mathbf{A}$ contains their coefficients in equation 3; and $\mathbf{b}$ is the data vector that contains the traveltime residuals. If we set the slowness derivatives with respect to ε and δ to zeros, the system degenerates to single parameter tomography. Similarly, it can be tailored to invert for two of the three parameters only.

Regularization

Matrix $\mathbf{A}$ in equation 9 is sparse and nonsymmetric. Its least square solution can be found by solving the following system:

$$\mathbf{A^T Ax} = \mathbf{A^T b}, \quad (10)$$

where $\mathbf{T}$ represents the transpose of a matrix. Matrix $\mathbf{A^T A}$ is square, symmetric and positive definite, and the system of equations 10 can be solved using linear solvers, such as the conjugate gradient method. Normally, it is an ill-posed system, and there is not a definite solution solely on the basis of fitting the data. A regularization method is introduced by Tikhonov and Arsenin (1977) and variations to it have been developed, among them regularization with steering filters (Clapp et al., 2004), anisotropic regularization (Zhou et al., 2008), and spatially variant Gaussian smoothing regularization (Zhou et al., 2009). Some people also refer to regularization as model styling or shaping filters. By adding regularization to the system, we have an additional goal to fit the data with model characteristics that we desire.

The anisotropy parameters may have independent spatial variations. For example, it is often assumed that ε and δ fields are much smoother than the velocity. Thus, it is natural to apply independent regularization (or model styling) to each individual parameter. Let us define three vectors $\mathbf{x_s}$, $\mathbf{x_\varepsilon}$, and $\mathbf{x_\delta}$ for slowness, ε, and δ updates:

$$\mathbf{x}_s = [(\Delta s_{p0})_1, (\Delta s_{p0})_2 ..., (\Delta s_{p0})_n, 0, \ldots, 0, 0 \ldots 0]^{\mathbf{T}}, \quad (11)$$

$$\mathbf{x}_\varepsilon = [0, \ldots, 0, s_{p0}\Delta\varepsilon_1, s_{p0}\Delta\varepsilon_2, \ldots, s_{p0}\Delta\varepsilon_n, 0, \ldots, 0]^{\mathbf{T}}, \quad (12)$$

$$\mathbf{x}_\delta = [0, \ldots, 0, 0, \ldots, 0, s_{p0}\Delta\delta_1, s_{p0}\Delta\delta_2, \ldots, s_{p0}\Delta\delta_n,]^{\mathbf{T}}, \quad (13)$$

where

$$\mathbf{x} = \mathbf{x_s} + \mathbf{x_\varepsilon} + \mathbf{x_\delta}. \quad (14)$$

The objective function is defined as

$$\varphi = \|\mathbf{b} - \mathbf{Ax}\|^2 + \tau_s\|\mathbf{R}_s\mathbf{x}_s\|^2 + \tau_\varepsilon\|\mathbf{R}_\varepsilon\mathbf{x}_\varepsilon\|^2 + \tau_\delta\|\mathbf{R}_\delta\mathbf{x}_\delta\|^2, \quad (15)$$

where $\mathbf{R}_s$, $\mathbf{R}_\varepsilon$, and $\mathbf{R}_\delta$ are regularization operators for the anisotropy parameters $\mathbf{x}_s$, $\mathbf{x}_\varepsilon$ and, $\mathbf{x}_\delta$, respectively, and τ_s, τ_ε and, τ_δ are corresponding regularization factors. We try to minimize the objective function and the minimum is found by setting $\frac{\partial\varphi}{\partial\mathbf{x}} = 0$. Thus we can obtain the final equation system.

$$\mathbf{A^T Ax} + \tau_s\mathbf{R}_s^{\mathbf{T}}\mathbf{R}_s\mathbf{x}_s + \tau_\varepsilon\mathbf{R}_\varepsilon^{\mathbf{T}}\mathbf{R}_\varepsilon\mathbf{x}_\varepsilon + \tau_\delta\mathbf{R}_\delta^{\mathbf{T}}\mathbf{R}_\delta\mathbf{x}_\delta = \mathbf{A^T b}. \quad (16)$$

With independent regularization operators, the tomography can produce different degrees of smoothness for each anisotropy parameter update. Also, by adjusting regularization factors τ_s, τ_ε and, τ_δ, we have some leverage to control the tomographic backprojection. For example, we can adjust the regularization factors to limit updates to the current velocity model.

SYNTHETIC EXAMPLES

The proposed tomography method is tested on the 2D BP TTI model (http://www.freeusp.org/2007_BP_Ani_Vel_Benchmark/listing.html). We choose to work on the right side of the model in order to avoid the salt structures. The true anisotropic model is shown in Figure 1. In practice, the accuracy of reflection tomography depends on the accuracy of picking the moveout residuals. However, for testing purposes, the difference between the true and current models is used to calculate the true travetime residuals during ray tracing, thereby eliminating picking errors. In order to obtain high resolution models, the residuals are picked on a grid of 31.25 m × 100 m. Three experiments are conducted to invert for V_{p0}; V_{p0}, ε and δ; and V_{p0} and ε, respectively, in order to study

DOI:10.1190/geo2010-0395.1

their data fitting behaviors and the resolution of each parameter. The same regularization is applied for each update parameter and for all experiments. The initial velocity model consists of a constant velocity water layer followed by a model with a depth gradient of 0.3 s^{-1}. The initial ε and δ models have two layers, the isotropic water layer being followed by a constant anisotropic layer with $\varepsilon = 0.1$ and $\delta = 0.05$. Three iterations of tomographic updating are conducted for each experiment with smoothing constraints of 300 m in the horizontal direction and 100 m in the depth direction gradually reduced to 50 and 25 m, respectively. True symmetry axis information is used in all experiments and no muting is applied to the migration gathers.

The first experiment is to invert for V_{p0} only, keeping the simple initial ε and δ values unchanged. The inverted velocity model (Figure 2a) is very similar to the true model (Figure 1a) in shape. The detailed lateral velocity resolution in the vicinity of the faults on the right hand side of Figure 2a is particularly impressive, and may be the result of dense, error-free picks. A high resolution image of velocity errors (Figure 2b) is obtained by subtracting the updated velocity model from the true model. Basically, this shows that the updated velocity is too slow in the region where the assumed Thomsen anisotropy parameter values are higher than the actual values, and vice versa. Tomography compensates for the estimated errors in ε and δ with appropriate velocity updates. The gathers (Figure 3b) are flat in general. However, residuals are still seen at large offsets of some events and events below 7000 m show poor continuity. The gathers also indicate that the reflectors are at incorrect depths compared to the gathers migrated with the true model (Figure 3a).

The second experiment is to conduct a three-parameter joint tomography that inverts for V_{p0}, ε, and δ, simultaneously. Although the updated velocity model (Figure 4a) is similar to the true model (Figure 1a) in general, discrepancies do exist (Figure 5a) with the largest errors occurring in the isotropic layers. In contrast to the velocity, the updated ε and δ models (Figure 4b, 4c) show lower resolution. The gathers (Figure 3c) are nearly as flat as those migrated with the true model (Figure 3a), which confirms that the joint tomography fits data better. Depth errors for the reflectors,

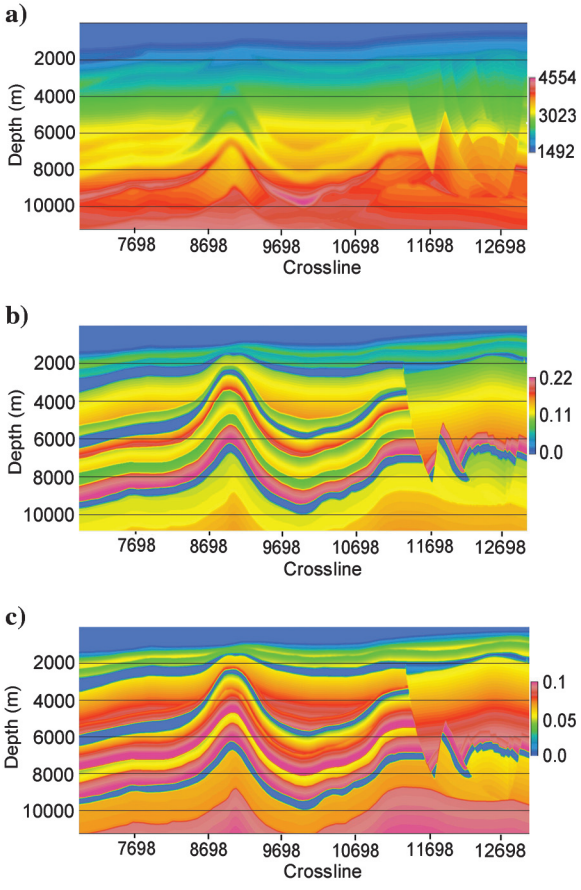

Figure 1. The true BP 2D TTI model: (a) velocity; (b) ε; (c) δ.

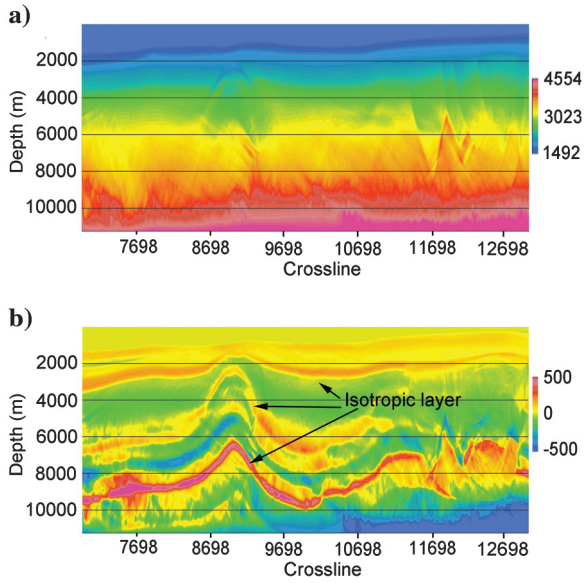

Figure 2. The velocity model updated from the single parameter tomography experiment compared with the true model: (a) the updated model; (b) the errors of the updated model. In the area below the water bottom and above 3000 m and in the isotropic layers, the updated model shows low velocities, coincident with the fact that the guessed ε and δ values are higher than the actual values. In most of the area below 3000 m, it shows higher velocities than the true values due to the fact that guessed ε and δ values are lower than the actual values.

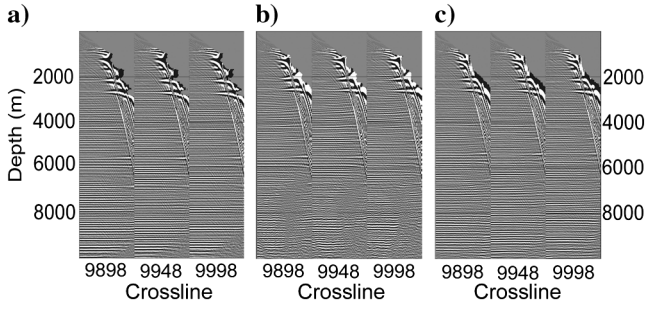

Figure 3. Gather comparison: (a) the gathers migrated with the true model; (b) the gathers migrated with the final model obtained from the single parameter tomography experiment; (c) the gathers migrated with the final model obtained from the three-parameter joint tomography experiment.

on the other hand, are still seen in Figure 3c. This experiment demonstrates that the joint tomography is nonunique and that there is ambiguity among the anisotropy parameters.

The last experiment uses the true δ model and inverts for V_{p0} and ε, with the objective of determining whether knowledge of the true δ values would help improve the accuracy of the results over the second experiment. The experiment achieves gather flatness, similar to that in the second experiment. As depicted in Figure 5, the updated V_{p0} and ε show at best only minimal error improvement. Generally speaking, ε shows smaller error magnitude wherever the velocity has smaller error magnitude, and vice versa. The velocity and ε the errors have opposite signs. Thus, the knowledge of δ does not eliminate the ambiguity between V_{p0} and ε.

Because the first two experiments have the same residual input and initial model at the beginning, a convergence comparison is conducted for the first round of tomographic updating between the single parameter tomography and the joint tomography for three parameters. The measurement of convergence is the percentage RMS misfit to the data. As expected, the joint tomography provides a better data fit (Figure 6), which conforms to the observation that the final gathers of the second experiment are flatter than those of the first experiment.

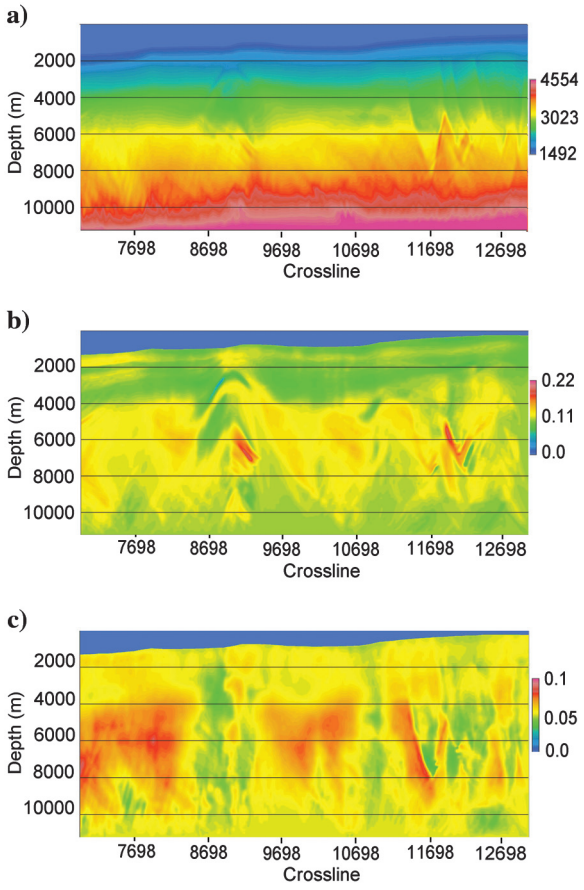

Figure 4. The final model from the three-parameter joint tomography experiment: (a) the updated velocity; (b) the updated ε; (c) the updated δ.

A FIELD TEST

The results here are for a 2D field data set acquired in the Gulf of Mexico. The acquisition shot interval is 37.5 m and the receiver interval is 12.5 m with 960 channels per shot. The maximum offset is 12 km. As shown in Figure 7a, there is a vertical well drilled at crossline 1560, with sonic data available between depths 3270 and 7272 m.

Because the tomographic inversion is nonunique, as shown in the synthetic examples, the well information must be used in order to obtain an anisotropic model that matches the well data. We decided

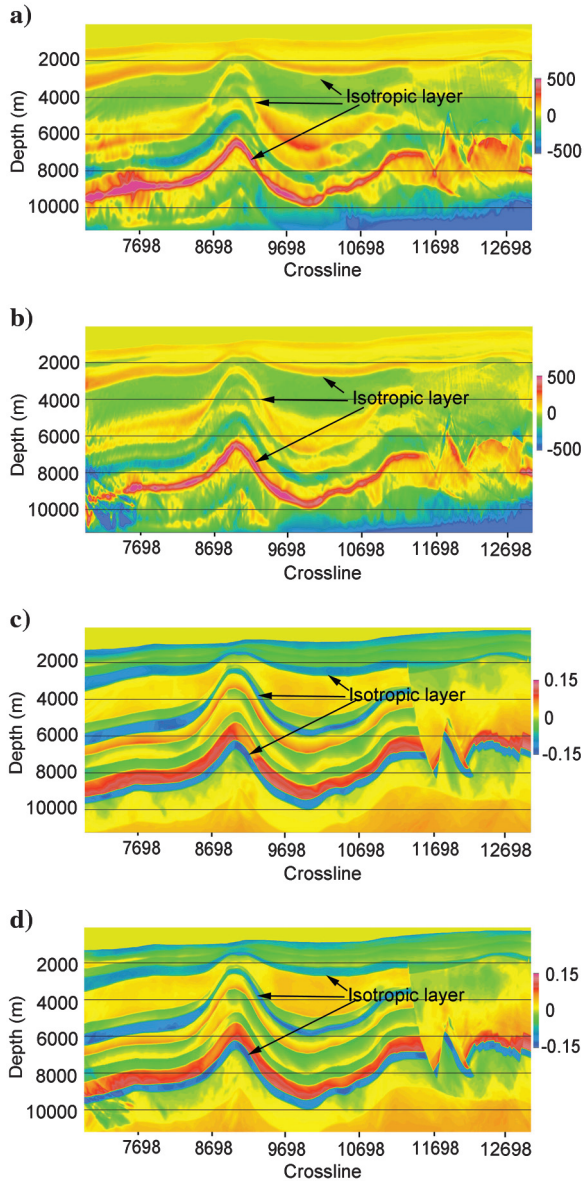

Figure 5. Model updating comparison between the three-parameter joint tomography experiment and the two parameter joint tomography experiments: (a) velocity errors of the three-parameter joint tomography experiment; (b) velocity errors of the two parameter joint tomography experiment; (c) ε errors of the three-parameter joint tomography experiment; (d) ε errors of the two parameter joint tomography experiment.

to construct the initial velocity model by extrapolating the velocity from the sonic data at the well location. Because the sonic data only provide information for a limited depth range, the first goal of model building is to obtain a close velocity estimate for the region above the geological layer (Figure 7a) where the sonic data start. It is achieved with the three-parameter joint tomographic updating using only the picks above the top Cretaceous reflector, about 1000 m below where the sonic data start. Although there are ways to estimate ε and δ for an initial anisotropic model (Gherasim et al., 2010), the three-parameter joint tomography is performed starting from an NMO velocity model with $\varepsilon = 0.0$ and $\delta = 0.0$. The symmetry axis information is assumed to follow the sediment beddings. Two iterations of tomography flatten the gathers and produce an anisotropic model. The resulting ε and δ estimates are directly used as initial values for a later tomographic updating. The sonic velocity is inserted into the corresponding depth range of the resulting velocity model at the well location. Then it is extrapolated, with the guide of the seismic image, over the whole model volume for the region, below the geological layer, where the sonic data start. This incorporated velocity model is then slightly smoothed and used as the initial velocity for later tomography.

This constructed velocity is assumed close to actual velocity so that during later tomographic updating, a "soft" control is applied on the velocity update by adjusting the regularization parameters to only allow small velocity changes. Consequently, most residuals are back projected to ε and δ updates. As shown in Figure 7b, the signal to noise ratio is very low, especially in the deep portion. Together with the limitation associated with 2D data, it implies a need for conservative updates. After five iterations of updates, the gathers (Figure 8b) are flat. The updated velocity model (Figure 9b)

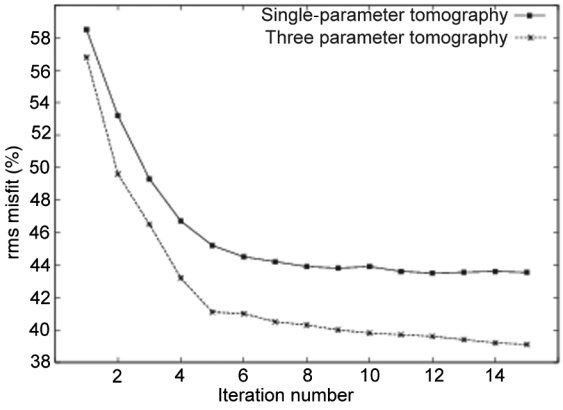

Figure 6. Data fit comparison between the single parameter tomography and the three-parameter joint tomography.

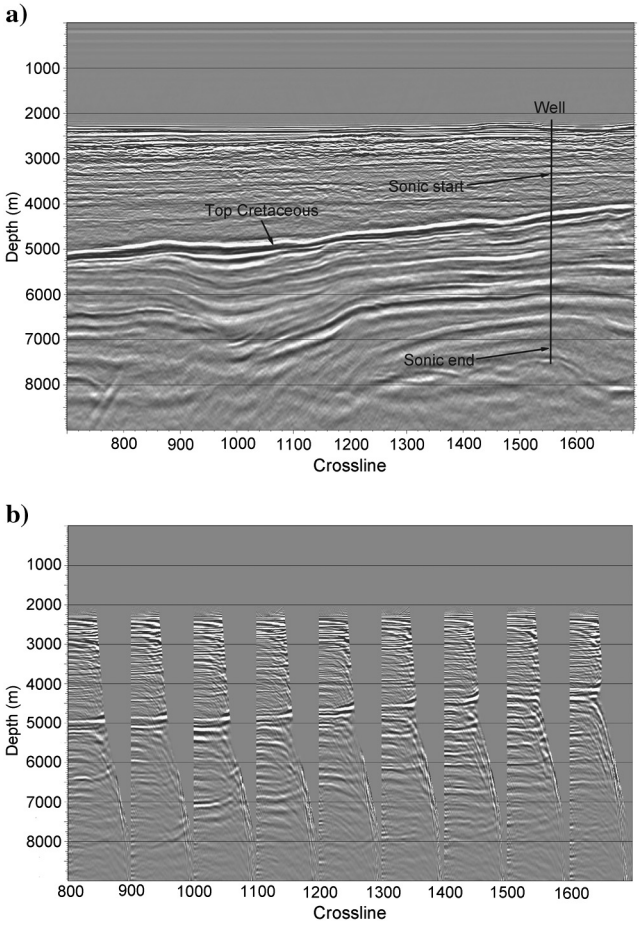

Figure 7. The migration stack and gathers with the NMO velocity model in the field data example: (a) the stack with the vertical well marked; (b) the gathers.

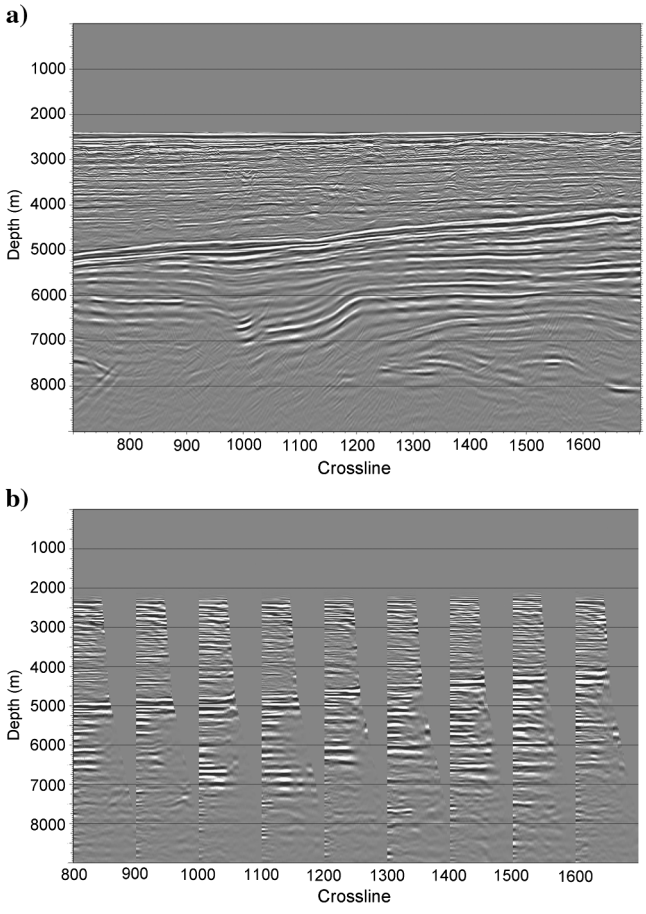

Figure 8. The final stack and gathers: (a) the stack; (b) the gathers.

changes only slightly compared to the constructed initial model (Figure 9a) and still matches the sonic data (Figure 10) at the well location. The inverted ε and δ (Figure 11) have reasonable values and the stack (Figure 8a) shows focused reflectors.

DISCUSSION

In the synthetic examples, we observe that single parameter tomography with a guess for ε and δ is inadequate for perfect seismic imaging. If we allow more degrees of freedom by simultaneously inverting for the perturbations of V_{p0}, ε and δ, the resulting model fits the data well and flattens the seismic gathers. However, the reflector depths are also normally in error due to the inaccurate velocity caused by the ambiguity among V_{p0}, ε and δ. With the knowledge of true δ, the ambiguity between ε and V_{p0} is still seen in the two parameter joint tomography. In general, if there is no information other than surface seismic data, there is ambiguity among all three anisotropy parameters. If one parameter can be determined, for example, from well data, the ambiguity still exists between the other two parameters.

An interesting observation in the joint tomography experiments is that the velocity has a better resolution than ε and δ. To investigate this issue, it is easier to start from the weak anisotropy approximation (Thomsen, 1986):

$$V = V_{p0}(1 + \delta \sin^2\theta \cos^2\theta + \varepsilon \sin^4\theta), \tag{17}$$

and equivalently,

$$s = s_{p0}(1 + \delta \sin^2\theta \cos^2\theta + \varepsilon \sin^4\theta)^{-1}. \tag{18}$$

Expanding equation 18 in a Taylor series and keeping only the linear terms yields

$$s = s_{p0}(1 - \delta \sin^2\theta \cos^2\theta - \varepsilon \sin^4\theta). \tag{19}$$

As previously mentioned, s_{p0} is bundled with $\Delta\varepsilon$ and $\Delta\delta$. The terms $\sin^2\theta\cos^2\theta$ and $\sin^4\theta$ make the slowness derivatives associated with ε and δ, and consequently the traveltime derivatives, smaller in magnitude than the derivative with respect to s_{p0}. They also imply that these derivatives are more sensitive to raypath changes. Thus, it is expected that ε and δ have a lower resolution, as confirmed by the synthetic experiments.

Reflection tomography is a data fitting problem with some resolution issues (Stork, 1992), and it is severely nonunique when three anisotropy parameters are simultaneously inverted, even with well

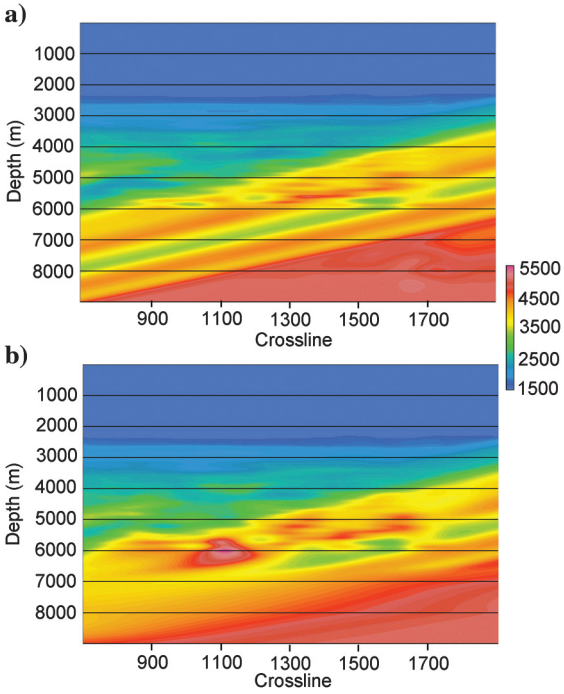

Figure 9. Velocity comparison: (a) the constructed initial velocity model; (b) the final model.

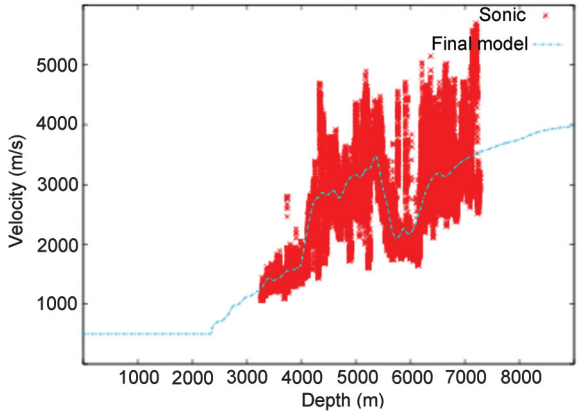

Figure 10. The velocity comparison at the well location between the final model and the sonic data.

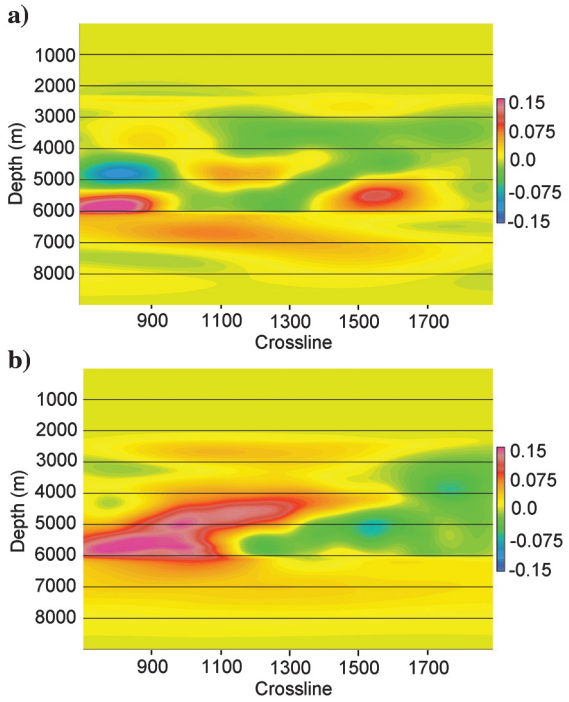

Figure 11. The final ε and δ models for the field data example: (a) ε; (b) δ.

DOI:10.1190/geo2010-0395.1

data (Bakulin et. al, 2010a). Joint tomography provides a way to get a better data fit, but it also adds more ambiguity to the problem. The joint tomography provides an anisotropic model that fits the data and has the model styling we wish, but this model may not be the true model. Additional information, such as well data, is critical to constrain the tomography, which is demonstrated in the field data test. In the field data example, the sonic velocity is extrapolated over the whole volume guided by the seismic image, and the resulting velocity model is assumed close to the correct velocity. Such an assumption may not be valid far away from the well, and some other way may need to be developed to constrain the tomographic inversion.

In all examples, the symmetry axis information is known or assumed to follow the sediment bedding. We have not addressed how errors in the symmetry axis affect the results. Theoretically, we can also formulate it into the tomography equations and invert for it. Then, we add more ambiguity and the system becomes even more nonunique.

CONCLUSIONS

We develop a multiparameter joint tomography method for TTI model building that can be used to invert for up to three anisotropic parameters simultaneously with or without well data. The synthetic experiments demonstrate that a single parameter tomography with guesses of ε and δ is inadequate for building the model for an anisotropic earth. The multiparameter joint tomography is more suitable for fitting data. However, there is ambiguity among the three anisotropy parameters, and it limits the resolution of each parameter. A reliable estimate of δ does not eliminate the ambiguity between the velocity and ε. Applying an independent regularization on each anisotropy parameter provides a way to constrain one parameter more than others. The field data example demonstrates such a regularization strategy and the importance of including well data as a constraint when estimating anisotropic models.

ACKNOWLEDGMENTS

We thank BP for providing the 2D TTI data set. We thank PGS for the permission to publish this paper. We thank our colleagues Boris Tsimelzon for preparing the field data, Don Heron for providing the well information, and Dan Whitmore for beneficial discussions and advice. We also thank all reviewers for their constructive comments and critiques.

REFERENCES

Alkhalifah, T., 1998, Acoustic approximations for processing in transversely isotropic media: Geophysics, **63**, 623–631.

Alkhalifah, T., and K. Larner, 1994, Migration error in transversely isotropic media: Geophysics, **59**, 1405–1418.

Alkhalifah, T., and I. Tsvankin, 1995, Velocity analysis in transversely isotropic media: Geophysics, **60**, 1550–1566.

Audebert, F. S., A. Pettenati, and V. Dirks, 2006, TTI anisotropic depth migration — Which tilt estimate should we use?: 68th Conference and Exhibition, EAGE, Extended Abstracts, 185.

Bakulin, A., Y. Liu, O. Zdraveva, and K. Lyons, 2010b, Anisotropic model building with wells and horizons: Gulf of Mexico case study comparing different approaches: The Leading Edge, **29**, no. 12, 1450–1460.

Bakulin, A., M. Woodward, D. Nichols, K. Osypov, and O. Zdraveva, 2010a, Building TTI depth models using localized anisotropic tomography with well information: Geophysics, **75**, no. 4, 27–36.

Bear, L. K., T. A. Dickens, J. R. Krebs, J. Liu, and P. Traynin, 2005, Integrated velocity model estimation for improved positioning with anisotropic PSDM: The Leading Edge, **24**, 622–634.

Bowling, J., S. Ji, D. Lin, M. Reasnor, M. Staines, and N. Burke, 2009, From isotropic to anisotropic: Puma/Mad Dog wide azimuth data case study: 79th Annual International Meeting, SEG, Expanded Abstracts, 246–250.

Cai, J., Y. He, Z. Li, B. Wang, and M. Guo, 2009, TTI/VTI anisotropy parameters estimation by focusing analysis, Part I: theory: 79th Annual International Meeting, SEG, Extended Abstracts, 301–305.

Clapp, R. G., B. L. Biondi, and J. F. Claerbout, 2004, Incorporating geologic information into reflection tomography: Geophysics, **69**, 533–546.

Gherasim, M., J. Etgen, B. Nolte, I. Ahmed, and G. Xia, 2010, Anisotropic velocity model building using OBS node tomography at Atlantis field, Gulf of Mexico: 80th Annual International Meeting, SEG, Expanded Abstracts, 4359–4363.

Grechka, V., and I. Tsvankin, 1998, Feasibility of nonhyperbolic moveout inversion in transversely isotropic media: Geophysics, **63**, 957–969.

Harlan, W. S., 1995, Regularization by model reparameterization: http://www.billharlan.com/pub/papers/regularization.pdf, accessed March, 2007.

Huang, T., S. Xu, and Y. Zhang, 2007, Anisotropy estimation for perstack depth migration — A tomographic approach: 77th Annual International Meeting, SEG, Expanded Abstracts, 124–128.

Jiang, F., H. Zhou, Z. Zou, and H. Liu, 2009, 2D Tomographic velocity model building in tilted transversely isotropic media: 79th Annual International Meeting, SEG, Expanded Abstracts, 4024–4028.

Jiao, J., S. Lin, C. Zhou, S. Brandsberg-Dahl, K. Schleicher, and H. Tieman, 2009, Multi-parameter controlled automatically picking and variable smoothing for tomography with fast 3D beam prestack depth migration: 79th Annual International Meeting, SEG, Expanded Abstracts, 3989–3993.

Koren, Z., I. Ravve, G. Gonzalez, and D. Kosloff, 2008, Anisotropic local tomography: Geophysics, **73**, no. 5, VE75–VE92.

Kosloff, D., U. Zackhem, and Z. Koren, 1997, Subsurface velocity determination by grid tomography of depth migrated gathers: 67th Annual International Meeting, SEG, Expanded Abstracts, 1815–1818.

Schleicher, K., J. Cramer, C. Gerrard, J. Jiao, S. Lin, A. Sosa, and C. Zhou, 2010, Model building for tilted transverse anisotropic depth migration of the Craystal Gulf of Mexico wide azimuth survey: 72nd Conference and Exhibition, EAGE, Expanded Abstracts, 253.

Stork, C., 1992, Reflection tomography in the postmigrated domain: Geophysics, **57**, 680–692.

Thomsen, L., 1986, Weak elastic anisotropy: Geophysics, **51**, 1954–1966.

Tikhonov, A. N., and V. Y. Arsenin, 1977, Solution of ill-posed problems: Winston & Sons.

Tsvankin, I., 2001, Seismic signatures and analysis of reflection data in anisotropic media: Elsevier.

Tsvankin, I., and L. Thomsen, 1995, Inversion of reflection traveltimes for transverse isotropy: Geophysics, **60**, 1095–1107.

Woodward, M. J., D. Nichols, O. Zdraveva, P. Whitfield, and T. Johns, 2008, A decade of tomography: Geophysics, **73**, no. 5, VE5–VE11.

Zhou, C., S. Brandsberg-Dahl, and J. Jiao, 2009, A continuation approach to regularize the reflection tomography with a 3D Gaussian filter: 71st Conference and Exhibition, EAGE, Expanded Abstracts, U031.

Zhou, C., J. Ramos-martinez, S. Lin, J. Jiao, and S. Brandsberg-Dahl, 2008, True geometry tomography for velocity model building with applications to WATS seismic data: 78th Annual International Meeting, SEG, Expanded Abstracts, 3260–3264.

Zhou, H., D. Pham, S. Gray, and B. Wang, 2003, 3D tomographic velocity analysis in transversely isotropic media: 73rd Annual International Meeting, SEG, Expanded Abstracts, 650–653.